Effect of pectin extraction method on properties of cellulose nanofibers isolated from sugar beet pulp

Mohammad L Hassan
National Research Centre
Linn Berglund
Lulea University of Technology: Lulea Tekniska Universitet
Wafaa S Elseoud
National Research Centre
Enas A Hassan
National Research Centre
Kristiina Oksman (kristiina.oksman@ltu.se)
Luleå University of Technology https://orcid.org/0000-0003-4762-2854

Research Article

Keywords: Sugar beet pulp, cellulose nanofibers, acid hydrolysis, enzymatic hydrolysis, cellulases, xylanases

Posted Date: June 24th, 2021

DOI: https://doi.org/10.21203/rs.3.rs-518873/v1

Abstract

In this study, the effect of pectin extraction method on the properties of cellulose nanofibers (CNFs) isolated from sugar beet pulp (SBP) was studied. Pectin was extracted by the industrially practiced method by sulfuric acid hydrolysis or by enzymatic hydrolysis using a cellulase/xylanase enzymes mixture. The CNFs were then isolated by high-pressure homogenization and investigated in terms of their chemical composition, crystallinity, size, degree of polymerization, and re-dispersion in water after freeze-drying. The mechanical properties and surface characteristics of CNFs films were also studied. The results showed that fibrillation of the de-pectinated SBP was more efficient for the acid hydrolyzed SBP. CNFs from the acid-hydrolyzed SBP had a slightly wider diameter, higher crystallinity, viscosity, and α-cellulose content but a lower degree of polymerization than CNFs from the enzyme-hydrolyzed SBP. Owing to the presence of more residual hemicelluloses in the CNFs from the enzyme-hydrolyzed SBP, the CNFs had higher re-dispersion ability in water. CNFs films from enzyme-hydrolyzed SBP displayed slightly better mechanical properties and higher water contact angles than acid-hydrolyzed CNF films.

Introduction

Sugar beet pulp (SBP) is a common agricultural residue in different areas of the world as 20% of the world production of sugar comes from sugar beets (Stevanato et al. 2019). Sugar beets are cultivated in Europe, North and South America, Asia, and a few countries in Africa where temperate climates exist. The top producer is the Russian Federation, followed by France, the United States, Germany, and Turkey. In Africa, Egypt is the leading country in sugar beet cultivation and the 8th top producer in the world. After sugar extraction, SBP residue is rich in some carbohydrate polymers and other minor components. The chemical composition of SBP is approximately 21–30% pectin, 22–25% cellulose, 22–25% hemicelluloses, 5–10% protein, lignin < 5%, phenolics < 1%, and ash < 1% (Fishman et al. 2011; Li et al. 2014).

Indeed, the cell wall structure of sugar beet is quite unique and different from those of agricultural residues such bagasse, rice straw, etc. Most of the tissue in sugar beet is parenchymal, which is separated by vascular tissue (Dinand et al. 1999). The parenchymal tissue is characterized by only primary wall of very thin thickness (as low as 0.1 μm). The inter-vascular parenchyma consists of arrays of ovoid cells having diameters ranging from 50 to 200 μm. Other parenchymal cells also exist in the vascular tissue, so called phloem parenchyma, and characterized by very thin wall with an elongated structure, with diameter of 0.4 μm and lengths of around 100 μm. Similar to the primary walls in different plants, the thin walls of the different parenchymal cells contain loosely organized cellulose microfibrils embedded in a matrix of hemicelluloses and pectin. The cellulose microfibrils are either isolated with about 3 nm diameter or organized in thin bundles with a limited number of parallel microfibrils (Dinand et al. 1999). This loose microfibrillar organization in the matrix facilitates separation of cellulose microfibrils by mechanical action.

Regarding hemicelluloses in SBP, they consist of two main polysaccharides xylan and xyloglucan (Kato and Kobayashi, 2000). The xylan polymer is a linear xylopyranosyl backbone with side chains of pentoses and hexoses sugars such as rhamnose, arabinose, glucose, galactose, and glucouronic sugars. Xylan part represents about 89% hemicelluloses in sugar beet pulp. On the other hand, the xyloglucan polymer consists of glucosyl backbone with side chains of xylopyranosyl, galactopyranosyl - xylopyranosyl, and fucopyranosyl-galactopyranosyl- xylopyranosyl sugar residues. Pectin consists of two main structural elements, homogalacturonan (HG) and rhamnogalacturonan (RG). HG and RG elements are linked to each other's via different kinds of bonds (Vincken et al. 2003; Schols et al. 2009). The HG consists of linear chains of d-galacturonic acid units, which are partially acetyl-esterified and methyl-esterified at *O*-2 and/or *O*-3 and at *O*-6, respectively (Combo et al. 2013). On the other hand, RG consists of rhamnose and galacturonic acid units arranged in alternating fashion. The rhamnose units are anchored with linear galactan and branched arabinan sugars. In addition to the polysaccharides in pectin structure, protein and ferulic acid residues exist linked to the arabinan and galactan side chains of the RG elements (Levigne et al. 2002; Siew and Williams, 2008).

In such a uniquely complicated cell wall structure of SBP, hemicelluloses are linked to pectin via formation of ester bonds with the hydroxyl and carboxylic groups of the later (Fischer et al. 1994). Cellulose microfibrils on the other hand are linked to pectin in the cell wall in similar manner to that with hemicelluloses (Zykwinska et al. 2005; Zykwinska et al. 2007).

For efficient use of SBP residue, industrially valuable polymers such as pectin and cellulose should be isolated using optimized protocols. Pectin extraction from the cell wall of sugar beet requires breaking the bonds between cellulose, hemicellulases, and pectin. Although hydrolysis using mineral acids is a common industrial method for pectin extraction, other methods, such as enzymatic hydrolysis, have also been studied (Zykwinska et al. 2008; Concha et al. 2013; Babbar et al. 2016; Pacheco et al. 2019; Abou-Elseoud et al. 2021). In addition to being a more environmentally sound approach than mineral acid hydrolysis, enzymatic hydrolysis was also found to be effective in terms of pectin yield in these previous studies. After pectin extraction, the de-pectinated SBP becomes enriched with cellulose fibers, which can be used to isolate nanocellulose (cellulose nanofibers and nanocrystals), a substance known to have interesting mechanical, optical, and physical properties, making them applicable in several areas (Thomas et al. 2018). The isolation of CNFs from de-pectinated SBP has been studied in past years. In these studies, the main protocol was to first remove pectin from SBP by alkali treatment, then remove lignin by bleaching, and finally isolate CNFs from the purified pulp using high-pressure homogenizers (Leitner et al. 2007; Li et al. 2014; Pinkl et al. 2017). The use of mixtures of enzymes (pectinases, hemicellulases, amylase, and endo-glucanase) to purify the cellulose fraction from residual pectin after alkali treatment and bleaching of SBP was also studied. The purified pulp was then subjected to high-pressure homogenization by a microfluidizer to produce CNFs (Holland et al. 2019; Perzon et al. 2020). In a slightly different protocol to isolate CNFs, SBP was first treated with hot nitric acid solution three times, alkali treated three times, bleached with sodium chlorite/acetic acid, treated with ultrasonication, and finally subjected to high-pressure homogenization (Agoda-Tandjawa et al. 2010). CNFs from SBP were also isolated without the removal of pectin or other polysaccharides; only a bleaching step with sodium

chlorite/acetic acid was carried out, and the CNFs were isolated by high-pressure homogenization using a microfluidizer (Hietala et al. 2017); the isolated nanofibers contained significant amounts of pectin, which gave them high re-dispersion properties in water. CNFs from SBP were also isolated without chemical treatment by direct grinding using an ultrafine grinder followed by high-pressure homogenization (Vartiainen et al. 2015). Using a different approach, SBP was subjected to steam explosion pretreatment before bleaching and ultrasonic treatment to obtain CNFs (Yang et al. 2018).

Despite successful isolation of CNFs from SBP in the abovementioned studies, full use of the major components of SBP in industry, e.g., pectin and cellulose, is necessary for economic reasons to expand the traditional use of SBP for animal feed alone. Therefore, optimized isolation of pectin before using the cellulose fraction is mandatory. In addition, because different methods can be used for pectin extraction, the effect of these methods on the properties of isolated CNFs needs to be studied.

The aim of the current work was to study the differences in properties of CNFs isolated from SBP residues by first optimizing the pectin isolation using the conventional industrially-practiced sulfuric acid hydrolysis or enzymatic treatment with a mixture of xylanase/cellulase enzymes, and then using the de-pectinated SBP to isolate the CNFs. The study also focused on the progression of fibrillation using acid- and enzymatic-hydrolyzed SBP, the re-dispersion of the dried nanofibers, and the properties of CNF films prepared by casting.

Experimental

Raw material and reagents

SBP was kindly supplied by Alnubariah Company for Sugar, Alexandria, Egypt. The chemical composition of the SBP was determined according to standard methods of chemical analysis (Browning 1967) regarding α-cellulose, pentosans, lignin, and ash content. Galacturonic acid content was determined using *m*-hydroxybiphenyl reagent as previously described (Meseguer et al. 1998). Protein content was determined from the nitrogen content analysis by the Kjeldahl method (Sàez-Plaza et al. 2013), where protein content % = N% × 6.25. Cellulase from *Trichoderma longibrachiatum* (β-glucosidase powder, ≥ 1.0 unit/mg) and xylanase (Purified endo-β1→4)-xylanase powder, ≥ 2500 units/g) from *Thermomyces lanuginosus* were purchased from Sigma Aldrich Sweden AB (Stockholm, Sweden) and used as received. Regarding activity of the enzymes, one unit of cellulase enzyme liberates 1.0 μmole of glucose from cellulose in one hour at pH 5.0 at 37°C after 2 h incubation time, while one unit of xylanase liberates 1 μmole of reducing sugar measured as xylose equivalents from xylan per min at pH 4.5 at 30°C.

Sulfuric acid, hydrochloric acid, glacial acetic acid, sodium chlorite (technical grade 80%), sodium hydroxide, sodium thiosulfate, potassium bromate, potassium bromide, and citric acid were analytical grade chemicals purchased from Fisher Scientific U.K. Ldt (Loughborough, UK) and used as received.

Extraction of pectin by enzymatic hydrolysis

Pectin extraction by cellulase/xylanase enzymes mixture from SBP was carried out as previously published by Abou-Elseoud et al. (2021). A mixture of xylanase and cellulase in a 1:1.5 unit ratio was prepared in citrate buffer at 25 °C. SBP, previously ground to pass through a 40-mesh screen, was added to the enzyme mixture at a liquor ratio of 1:15 (SBP to enzyme mixture) at 50 °C under shaking at 150 rpm for 4 h. The enzymes were then inactivated by heating at 100 °C for 5 min. The residue (de-pectinated SBP) was separated from the soluble compounds by vacuum filtration and washed with distilled water. The de-pectinated SBP yield was calculated as follows:

De-pectinated SBP yield (%) = (oven-dry weight of SBP after extraction/oven-dry weight of SBP before extraction) × 100 (Eq. 1)

The filtrate was centrifuged at 10,000 rpm for 10 min to remove fine particles (fines), and pectin was precipitated by the addition of ethanol at volume ratio of 3:1 ethanol to filtrate. After 2 h, the precipitated pectin was centrifuged at 10,000 rpm for 20 min, washed with 70% ethanol, centrifuged again, and dried at 40 °C for 48 h. The pectin yield was calculated as follows:

Pectin yield (%) = (oven-dry weight of pectin/oven-dry weight of SBP) × 100 (Eq. 2)

Extraction of pectin by acid hydrolysis was carried out as previously published by Abou-Elseoud et al. (2021). SBP was suspended in water at a liquor ratio of 1:15 and acidified to pH 1 with sulfuric acid. The mixture was heated at 85 °C for 2 h under mechanical stirring of 500 rpm. The residue was then separated from the soluble compounds by vacuum filtration and washed with distilled water. The yield of the de-pectinated SBP was calculated according to Eq. 1. The filtrate was treated as mentioned in Sect. 2.2, and the pectin yield was calculated according to Eq. 2.

Isolation of cellulose nanofibers

After pectin extraction, the de-pectinated SBP samples were washed with water and then treated with diluted sodium hydroxide (4% based on de-pectinated SBP weight) at 25 °C under mechanical stirring for 1 h to remove residual solubilized pectin that was not removed by washing. Then, the mixture was filtered, and the produced pulp was washed with water until reaching neutral pH. The pulp was finally bleached with a sodium chlorite/acetic acid mixture at 80°C for 1 h (Wise et al. 1946).

To isolate the CNFs, the purified pulp, at 2 wt.% consistency, was mixed for 15 min in a Silverson L4RT shear mixer (Silverson Machines Ltd., Chesham, UK) followed by high-pressure homogenization using a two-chamber APV-2000 high-pressure homogenizer (SPX, Soeborg, Denmark). The pressure was maintained at 40 bar in one chamber and at 400 bar in the other chamber. The number of passes through the homogenizer varied from one to five times depending on the progression of fibrillation. The progression of the fibrillation was followed by measuring the viscosity at different passes/time through the homogenizer using a tuning-fork vibration viscometer Vibro Viscometer SV-10 (A&D Company Limited, Tokyo, Japan). The progression of fibrillation was also followed by optical microscopy using a polarizing microscope (Nikon Eclipse V100N POL, Tokyo, Japan) and the imaging software NIS-Elements D 4.30.

Characterization of isolated CNFs

The chemical composition of isolated CNFs was determined according to standard methods of analyses of α-cellulose, hemicelluloses (as pentosans), lignin, and ash content (Browning 1967). Galacturonic acid content was determined according to the previously published method using *m*-hydroxybiphenyl reagent (Meseguer et al. 1998). Protein content was determined from the nitrogen content analysis by the Kjeldahl method (Sàez-Plaza et al. 2013).

The microstructure of the SBP before and after pectin extraction was investigated using an FEI Quanta 200 scanning electron microscope (FEI Company, Eindhoven, The Netherlands). SBP samples were coated with gold prior to investigation using a sputtering coating system (Edwards Vacuum Engineering, Sussex, UK).

The microstructure of the isolated CNFs was studied using a high-resolution transmission electron microscope (TEM) (JEM-2100, JEOL, Tokyo, Japan). A drop of highly diluted CNF suspension (~ 0.02 wt.%) was placed on a copper grid bearing a carbon film. Phosphotungstic acid staining was applied to the sample after it has been air-dried, and left to dry before examination.

The isolated nanofibers were also examined using atomic force microscopy (AFM) to measure their size. Suspension with a concentration of 0.01 wt.% was dropped onto freshly cleaved mica for scanning with a Veeco Multimode Scanning Probe (Santa Barbara, CA, USA) in tapping mode using a tip model TESPA [antimony (n)-doped Si] (Bruker, Camarillo, CA, USA). Height scans were used to measure the width in air at 22°C using Nanoscope V software. The average values and standard deviations presented were based on 60 separate measurements.

For the testing of re-dispersion in water, 0.1 g of the freeze-dried CNFs was dispersed in 100 mL of de-ionized water and stirred with a magnetic stirrer for 10 min at 300 rpm. Last, ultrasonic treatment was applied for 1 min using a 400 Hielscher ultrasonic processor (Hielscher Ultrasonics GmbH, Teltow, Germany). A 1-cm-diameter probe was used at amplitude of 75%; the beaker was kept in ice water to avoid water evaporation. Light transmittance was measured immediately after ultrasonic treatment using a UV-visible spectrophotometer (Jenway 7205, Staffordshire, England) at 400–800 nm. The ultrasonic treatment was repeated at 1 min intervals, and light transmittance was measured until no noticeable change occurred. The total ultrasonic time used was 6 min for all samples. The freeze drying before the test was carried out as follows: the nanofibers suspensions (~ 2 wt.%) were stored in a freezer at a temperature of approximately − 20°C for at least 24 h prior to freeze-drying, which was conducted for 48 h using a freeze dryer (Alpha 2–4 LD Plus, CHRIST GmbH, Osterode am Harz, Germany) at a temperature of -40°C and a vacuum of 0.12 mbar.

The X-ray diffraction (XRD) patterns of CNFs were recorded using an Empyrean X-ray diffractometer (PANalytical, Netherlands). The crystallinity index (CrI) was calculated from the XRD patterns according to the following Eq. 3 (Sidiras et al. 1990; Segal et al. 1959):

$CrI = ((I_{002} - I_{am})/I_{002}) \cdot 100$ (Eq. 3)

where I_{002} is the intensity of the diffraction profile at the position of the 002 peak ($2\theta = 22.7°$) and I_{am} is the intensity of the minimum at approximately $2\theta = 18°$.

The degree of polymerization (DP) of the nanofibers was determined using the bis(ethylenediamine) copper(II) hydroxide solution method. Approximately 0.1 g was used in the test (Browning, 1967).

Characterization of CNF films

CNF films were prepared by casting CNF suspensions in a 9-cm-diameter Teflon petri dish. The suspensions were dried at 40°C for 18 h in an oven with circulating air. The produced films were conditioned at 50% relative humidity for 48 h at 25°C before testing.

The wettability of the CNF films was assessed by water contact angle measurements using an EASYDROP measuring system, drop shape analysis control (DSA1), and evaluation software (Krüss GmbH, Hamburg, Germany). A 4 mL water drop was released onto the sample surface, and its contact angle was measured by the sessile drop technique. The reported values are the average of six measurements for each sample.

The topographical features of the CNF films were studied using the same AFM setup described above, and the root-mean-square roughness was measured from the height scans. This was carried out to study the contribution of the topographical features to the contact angle measurement. Amplitude scans were also collected. The reported values are the average of seven measurements.

The mechanical properties were measured using a Lloyd instrument (LR10 K; Lloyd Instruments, Fareham, UK) with a 1 kN load cell at 25 °C using a crosshead speed of 2 mm/min. The sample width and length were 10 and 60 mm, respectively, and the distance between the grips was 20 mm. Five specimens from each sample were measured, and the results were averaged.

Results And Discussion

For effective use of the SBP residue, its pectin should be extracted first under optimized conditions. Pectin is an important food additive, and its isolation from the sugar beet should be carried out carefully to obtain the highest possible yield while maintaining its functional properties such as emulsification and gelling. After pectin extraction, the residual pulp has high cellulose content, which can be used to produce nanofibers with relatively low energy consumption. In the current work, pectin was extracted by sulfuric acid hydrolysis as it is practiced industrially or by enzymatic hydrolysis using a mixture of xylanase and cellulase enzymes; the conditions of pectin extraction by both methods were optimized in a previous publication to get highest pectin yield (Abou-Elseoud et al. 2021); the pulp residues after pectin extraction were used to isolate CNFs. In case of sulfuric acid extraction, the de-pectinated SBP residue was 43.1%, which was reached under extraction conditions of 85 °C for 2 h at pH 2. With enzymatic hydrolysis, the de-pectinated SBP residue was 61.4%, which was reached using a 1:1.5 xylanase to cellulase enzymes

mixture. The lower residual de-pectinated SBP with acidic extraction could have been owing to hydrolysis of more polysaccharides into water-soluble products than was the case when using enzymes.

Figure 1 shows SBP before and after pectin extraction. As shown in Figs. 1a to 1c, after pectin extraction from SBP by the acid or enzymes hydrolysis, most of the parenchymal tissues between and in the vascular bundles collapsed, and thus the characteristic vascular fibers bundles became clearly visible as in Figs. 1b and 1c. These vascular bundles de-folded at longer reaction times and under mechanical stirring. As Fig. 1d shows, the bundles have few microns diameter but hundred microns in length. The bundles contain cellulose microfibrils embedded in residual hemicelluloses and pectin. It is noted from the images that the vascular bundles obtained after pectin extraction by enzyme hydrolysis have more residual parenchymal tissue at their surfaces. In-deeds, after extraction pectin from the parenchymal tissue, the remained very thin cell wall contains the cellulose microfibrils and can easily be broken by mechanical action liberating the microfibrils or microfibrils bundles (Dinand et al. 1999).

Fibrillation of CNFs

The fibrillation progression of CNFs from the de-pectinated SBP by acid or enzymatic hydrolysis using high-pressure homogenization was measured using viscosity measurements and optical microscopy. Previous studies have shown that increased viscosity is a good measure of the progression of fibrillation as viscosity increases with increasing fibrillation (Berglund et al. 2020; Hassan et al. 2018). This increase in viscosity is due to an increase in the surface area and the high-water binding capacity of the isolated nanofibers. As shown in Fig. 2, the viscosity of the acid hydrolyzed SBP suspension increased very rapidly during the first pass of homogenization, followed by a decrease; the maximum viscosity was 280 mPa·s after the first pass. The temperature increased from 25.5 to 43 °C after two passes, which could also cause a decrease in the measured viscosity. The viscosity of the enzyme hydrolyzed SBP residue increased to a much less extent and reached a maximum after five passes; the maximum viscosity was 55 mPa·s and the temperature reached 43 °C. These results indicate faster isolation of CNFs when using the acid hydrolyzed SBP residue.

These results were also confirmed by optical microscopy images taken during the high-pressure homogenization. These images are shown in Figs. 3 and 4 for the acid-hydrolyzed and enzyme-hydrolyzed SBP, respectively. The micrographs show faster disappearance of the micro-sized fibers bundles and also the non-fibrous very thin-walled flatten parenchyma cells in the ground of the image (Figs. 3a) of the acid-hydrolyzed SBP than with the enzymatic hydrolysis (Fig. 4a). Upon high-pressure homogenization, the nonfibrous parenchymal cells disappeared, as well as the micro-sized cellulose fibers, which disintegrated into nano-sized fibrils.

The difference in the progression of fibrillation and viscosity values could be interpreted from chemical analyses of SBP and the nanofibers as seen in Table 1. SBP contains mixture of different polymers mainly pectin, cellulose, and hemicelluloses exist in very complex structure and connected together via different kinds of bonds. Hemicelluloses in SBP consist mainly of xylan (~ 89%) and xyloglucan

polymers (Kato and Kobayashi 2000) as mentioned in the Introduction. These hemicelluloses are chemically linked to pectin through ester bonds with pectin (Fischer et al. 1994). Cellulose microfibrils in SBP are linked to pectin in the cell wall in similar way to that of hemicelluloses (Zykwinska et al. 2005; Zykwinska et al. 2007). Evidence also exists regarding linkages between pectin, hemicelluloses, and cellulose via hydrogen and chemical bonding (Fry 1986; Iiyama et al. 1994). Therefore, extraction any of these components depends on cleaving the links between these polysaccharides. In addition to the aforementioned polymers in SBP, considerable amount of protein exists in SBP which is linked to pectin (Levigne et al. 2002; Siew and Williams 2008).

As shown in Table 1, after pectin extraction by acid or enzymatic hydrolysis followed by bleaching of SBP, higher α-cellulose content (~ 88%) was found with the acid-hydrolyzed SBP than with the enzyme-hydrolyzed SBP (~ 77%). This means that with the acid hydrolyzed SBP, removal of most of the hemicelluloses and pectin, which are chemically linked to cellulose fibers (Fry 1986; Iiyama et al. 1994) took place resulting in easier fibrillation and much faster increase in viscosity. The hemicelluloses content (estimated as pentosans) was ~ 7.0% and 17% for CNFs from the acid- and enzyme-hydrolyzed SBP, respectively. It is important to mention that pectic substance in SBP contains also pentose sugars (arabinose). Residual pectic substance in the nanofibers, determined as galacturonic acid, was 2.44% and 2.21% in case of acid- and enzyme-hydrolyzed CNFs, respectively, compared to ~ 19% in the SBP. It should be also noted that pectic substance in SBP consists of galacturonic backbone, in addition to branches of galactan and arabinan from the rhamnogalacturonan units (Schols et al. 2009).

The higher viscosity at the end of fibrillation for the acid-hydrolyzed SBP than for the enzyme-hydrolyzed SBP could be attributed to the higher cellulose content of the former, i.e., more nanofibers were liberated in the water suspension by high-pressure homogenization. In fact, hemicelluloses and pectin in SBP have low molecular weight and viscosity, and thus their presence in the isolated nanofibers is not expected to considerably affect the viscosity of the CNF suspension. The presence of residual pectin with nanofibers isolated from SBP was reported in a previous publication, despite the strong alkali extraction used in these previous studies (Perzon et al. 2020). Owing to the bleaching of SBP, traces of lignin were detected in both types of nanofibers (0.5%). The DP of cellulose was 639 and 894 for nanofibers isolated from the acid- and enzyme-hydrolyzed SBP, respectively. The lower DP of the nanofibers from the acid hydrolysed SBP was more likely owing to more degradation by the action of the acid during pectin extraction than that in case of using the enzymes.

Table 1
Chemical composition of sugar beet pulp (SBP) and the isolated CNFs

Materials	α-Cellulose (%)	Pentosans (%)	Galacturonic acid (%)	Lignin (%)	Protein content (%)	Ash (%)
SBP	38.02 ± 2.24	18.20 ± 2.12	19.40 ± 1.27	3.85 ± 0.21	10.13 ± 0.93	2.77 ± 0.42
CNF from acid-hydrolyzed SBP	87.80 ± 3.60	6.96 ± 0.79	2.44 ± 0.47	0.45 ± 0.16	0.31 ± 0.01	1.10 ± 0.08
CNF from enzyme-hydrolyzed SBP	76.90 ± 1.60	17.09 ± 1.39	2.21 ± 0.19	0.52 ± 0.5	0.25 ± 0.02	1.21 ± 0.05

Microstructure of isolated CNFs

Regarding the dimensions of the isolated nanofibers, TEM images showed that the diameters of the nanofibers isolated from both types of SBP residue were very homogenous. The diameters were 6–10 nm and 3–5 nm for nanofibers isolated from acid- and enzyme-hydrolyzed SBP, respectively (Figs. 5a and 5b, respectively). This means that elementary cellulose fibrils could be easily isolated from both types of SBP residue using high-pressure homogenization after one and five passes through the homogenizer for acid- and enzyme-hydrolyzed SBP, respectively. The length of the nanofibers was several microns for both types of SBP residue. AFM images confirmed the trend of the diameter of isolated nanofibers for both types of SBP residue; the measured widths were 10 ± 5 nm and 7 ± 4 nm for the acid- and enzyme-hydrolyzed SBP, respectively (Figs. 5c and 5d, respectively). The size distribution of isolated CNFs measured from AFM height scans is shown in Supplementary Information Figure S1.

A comparison of the diameter of SBP nanofibers in the current work to that in other publications is shown in Table 2. The diameter of CNFs obtained in the current work was among the smallest, and more interestingly, that for the acid hydrolyzed SBP was reached after only one pass through the high-pressure homogenizer. Other studies where similar widths of CNFs were isolated from SBP required many passes through high-pressure homogenizers (Agoda-Tandjawa et al. 2012; Pinkl et al. 2017) or the use of many enzymes plus many passes through the homogenizers (Perzon et al. 2020).

Table 2
Comparison between sizes of CNFs isolated from SBP residue in the current work and in previous publications under the conditions indicated

Pectin extraction	Purification process	Fibrillation	Size (nm)	Ref.
Sulfuric acid pH 1, 85 °C, 2 h	Dilute alkali, 25 °C, bleaching	High-pressure homogenizer 1 pass	6–10	Current work
Xylanase/cellulase enzymes pH 5, 50 °C,4 h	Dilute alkali, 25 °C bleaching	High-pressure homogenizer 5 pass	3–5	Current work
Alkali treatment 80 °C, 2 h	Bleaching	Microfluidizer 11 pass	20–40	Perzon et al. 2020
Mixture of enzymes	Bleaching	Microfluidizer 11 pass	~ 5	¨
Alkali treatment 80 °C, 2 h & mixture of enzymes	Bleaching	Microfluidizer 11 pass	20–40	¨
Homogenization, pH 9, 2 h & mixture of six enzymes 40°C for 24 h	None	Microfluidizer 18 min	5	Holland et al. 2019
None	Bleaching	Steam explosion/ultrasonic treatment	10–50	Yang et al. 2018
Alkali treatment 82 °C, 2 h None	Bleaching Bleaching	Microfluidizer 5 passes	≤100 ≤100	Hietala et al. 2017
Alkali treatment, 80 °C, 2 h	Bleaching	High-pressure homogenizer 20 passes	5–10	Pinkl et al. 2017
Alkali treatment, 80 °C, 2 h	Bleaching	High-pressure homogenizer 10 passes	10–70	Li et al. 2014

* Estimated from the scale bar on the TEM image since the actual diameter was not mentioned.

Pectin extraction	Purification process	Fibrillation	Size (nm)	Ref.
Nitric acid, 0.1 N, 85°C, 30 min, repeated 3 x Alkali 80 °C, 0.5 h, repeated 3 x	None	Ultrasoniction & high-pressure homogenizer 65 °C and 10 passes	2–15	Agoda-Tandjawa et al. 2010
Alkali treatment 80 °C, 2 h	Bleaching	High-pressure homogenizer 10–15 passes	30–100	Leitner et al. 2007
Alkali treatment, 80 °C, 2 h	Bleaching	High-pressure homogenizer, 65 °C 15 passes	≤20*	Dinand et al. 1999
* Estimated from the scale bar on the TEM image since the actual diameter was not mentioned.				

Crystallinity

The XRD patterns of CNFs isolated from acid- and enzyme-hydrolyzed SBP residues are shown in Fig. 6. Both types of CNFs have a cellulose I structure, namely, peaks at 22.5° and 16°, which correspond to diffraction from the (200) and (110) planes, respectively (French et al. 2014). The calculated crystallinity index from the differration patterns (Supplementary Information Figure S2) was higher for CNFs isolated from acid-hydrylyzed SBP (79%) compared to that for CNFs isolated from enzyme-hydrolyzed SBP (73%). The higher crystallinity of the acid-hydrolyzed CNFs means that the acid method was more effective in dissolving the amorphous parts of cellulose and hemicelluloses during pectin extraction. This is in accordance with the chemical analysis results mentioned previously. Another peak of low intensity at 2θ = 7.2° appeared in the pattern, which could be assigned to residual pectin (Wathoni et al. 2019), which was higher in case of the CNF isolated from the acid-hydrolyzyed SBP than that isolated from the enzyme-hydrolyzed SBP.

Redispersion of freeze-dried CNFs

The redispersion of dried CNFs is a challenge because of the strong aggregation of the nanofibers by extensive hydrogen bonding upon drying. Previous studies on nanofibers isolated from untreated SBP (without pectin removal) showed the possibility of redispersing the dried nanofibers in water into individual nanofibrils up to 80% of the dried nanofibers (Hietala et al. 2017). This was attributed to the presence of residual pectin and hemicelluloses attached to the isolated nanofibers. In the current study, redispersion of freeze-dried CNFs isolated from acid- and enzyme-hydrolyzed SBP was tested using light transmittance measurements (Kangas et al. 2014). Cellulosic nanofibers isolated by chemical-mechanical treatment as in the current work form colloidal suspensions with good transparency because of their nano-dimensions, whereas aggregates of microfiber size are opaque and white. Theoretically, the

finer the nanofibers, the higher the transparency of the suspension owing to the higher light transmittance.

As shown in Fig. 7, the non-dried CNFs from the acid- and enzyme-hydrolyzed SBP had very close light transmittance owing to their close diameters, as shown above in the AFM and TEM images. Upon freeze-drying and redispersion in water, the CNFs isolated from the enzyme-hydrolyzed SBP showed much higher light transmittance than the CNFs isolated from the acid-hydrolyzed SBP, i.e., the CNFs isolated from the enzyme-hydrolyzed SBP showed greater redispersion. This could be attributed to the higher hemicelluloses content and pectin residues in CNFs isolated from the enzyme hydrolyzed SBP.

The presence of these non-cellulosic residues hinders aggregation of the nanofibers upon drying. At 800 nm (the highest light transmittance obtained), freeze-dried CNFs from enzyme-hydrolyzed SBP retained 90% light transmittance after redispersion in water as compared to the non-dried CNFs, whereas freeze-dried CNFs isolated from acid-hydrolyzed SBP retained only 51% light transmittance. The presence of aggregates after redispersion of the CNFs was clearly seen in the optical microscopy images, which show many more aggregates for the redispersed CNFs isolated from acid-hydrolyzed SBP (Fig. 8).

CNF films

Films made by casting CNFs suspensions were prepared and their surface properties were characterized using water contact angle measurements and AFM. Their mechanical properties were also investigated.

Topography and wettability of CNF films

Figure 9 shows the captured AFM scans, where the root-mean-square roughness was measured from the height images to evaluate any contribution of the topographical features to the contact angle measurements. Furthermore, amplitude images of a smaller scan area were captured to visualize the topography characteristics. Water contact angles are also displayed to compare the wettability behavior of the CNFs films from acid- and enzyme-hydrolyzed SBP.

The topography of the CNFs films showed similar characteristics, with intertwined yet visually distinguishable nanofibers and spherical particles, as shown in Figs. 9c and 9d. The roughness of the film surfaces was measured to be 81 ± 6 and 76 ± 6 for CNFs isolated from acid- and enzyme-hydrolyzed SBP, respectively. CNF films isolated from acid-hydrolyzed SBP displayed slightly higher wettability, with a water contact angle of 56 ° ± 1.9, whereas that of enzyme-hydrolyzed SBP was 61 ° ± 1.3 (Figs. 9a and 9b, insets). It is well known that the water contact angle correlates with the topographical structure of the surface (Herrera et al. 2014). In addition, the wettability of cellulosic surfaces toward water has previously been reported to decrease upon the reduction of hemicelluloses for wood (Hosseinaei et al. 2011) and with the reduction of hemicelluloses and pectin for CNFs from carrot residue (Berglund et al. 2020). In the current work, although CNFs isolated from enzyme-hydrolyzed SBP had more hemicelluloses than those isolated from acid-hydrolyzed SBP, films from the latter had a slightly higher water contact angle. This

could be owing to the higher roughness of the surface of the CNF films isolated from the acid hydrolyzed SBP.

Mechanical properties CNF films

The tensile strength properties (maximum tensile strength, Young's modulus, and strain at maximum load) of CNFs films prepared from both types of isolated nanofibers were measured. Stress–strain curves for representative samples are shown in Supplementary Information Figure S 3. CNFs films isolated from acid- and enzyme-hydrolyzed SBP had close tensile strength values (49 ± 5 and 52 ± 6 MPa, respectively). Young's modulus was 2.4 ± 0.3 and 2.8 ± 0.6 GPa and strain was 4.5 ± 0.8% and 2.8 ± 0.6%, for nanofibers isolated from acid- and enzyme-hydrolyzed SBP, respectively. This higher Young's modulus could be owing to the higher DP of nanofibers from the enzyme hydrolyzed SBP. The DP values for CNFs isolated from enzyme- and acid-hydrolyzed SBP were 639 and 894, respectively.

The relatively lower mechanical properties of CNF films in the current study as compared to those reported in previous studies could be attributed to the following reasons. One of the reasons could be the method of drying of the film since free drying (without applying pressure) could result in lower tensile strength properties of CNF films. In addition, in the current study, acid hydrolysis (pH adjusted to 1) and cellulases enzymes were used in the extraction of pectin. This have resulted in greater degradation of the cellulose chains than in other studies where alkali treatment was used to remove pectin (Leitner, Hinterstoisser, Wastyn, Keckes, & Gindl, 2007; Hietala, Sain & Oksman, 2017; Pinkl, Veige, Colson, & Gindl-Altmutter, 2017; Perzon, Jørgensen, & Ulvskov, 2020). Alkali treatment conditions used in the previous studies removed almost all pectin, hemicelluloses, and short-chain cellulose, and thus there was a lower possibility of degrading cellulose than when using acid or cellulase enzymes. In addition, in one of these studies (Hietala, Sain & Oksman, 2017), the films from the isolated nanofibers were prepared by hot pressing at elevated temperatures (110 °C and 11 MPa pressure for 30 min), whereas those prepared in the current work were dried without pressure.

Conclusions

This study has shown that the removal of pectin using sulfuric acid- or xylanase/cellulase enzymatic hydrolysis leads to a residue with a high cellulose content and thus to a suitable raw material for CNFs production. The progression of CNFs isolation from de-pectinated SBP and the width of the isolated CNFs was dependent on the method of extracting pectin. CNFs with homogenous widths similar to those of elementary cellulose fibrils (approximately 5–10 nm) from SBP de-pectinated using sulfuric hydrolysis were easily isolated after one pass through a high-pressure homogenizer, whereas five passes were needed for enzyme de-pectinated SBP. Under the conditions used in this study, the extraction of pectin with sulfuric acid removed most of the hemicelluloses and pectin, resulting in easier fibrillation of cellulose fibers than was the case when extracting pectin with enzymes. However, the presence of more residual hemicelluloses for CNFs isolated from enzyme-hydrolyzed SBP resulted in higher redispersion of the freeze-dried nanofibers for CNFs isolated from acid-hydrolyzed SBP. Because of the greater degradation of cellulose during pectin extraction for the acid-hydrolyzed SBP, the prepared films had a

lower tensile modulus than those for the enzyme-hydrolyzed SBP. Finally, comparing the mechanical properties of CNFs films in the current study to those previously published ones, where pectin was removed mainly by alkali treatment, the extraction of pectin from SBP by industrially practiced mineral acid hydrolysis or by using cellulase enzymes resulted in nanofibers with lower mechanical properties than in the case of using alkali treatment in pectin extraction.

Declarations

Acknowledgments

This research was funded by the Swedish Research Council (Project No. 2015-05847) and received financial support from Bio4Energy, a strategic research environment appointed by the Swedish government; Swedish Foundation for Strategic Research within the HEALiX project (RMX18-0039), Kempe Foundations for the use of AFM, and Science and Technology Development Fund (STDF, Egypt, Project No. 25848).

Ethics declarations

Conflicts of Interest

The authors declare no competing interests.

Human or animal experiments

Not applicable

Additional information

Availability of materials and data

All data generated or analyzed during this study are included in this published article (and its Supplementary Information files).

References

1. Abou-Elseoud WS, Hassan EA, Hassan ML (2021) Extraction of pectin from sugar beet pulp by Enzymatic and ultrasound-assisted treatments. Carbohydrate Polymer Technologies Applications 2:100042
2. Agoda-Tandjawa G, Durand S, Berot S, Blassel C, Gaillard C, Garnier C, Doublier J-L (2010) Rheological characterization of microfibrillated cellulose suspensions after freezing. Carbohydr Polym 80:677–686
3. Agoda-Tandjawa G, Durand S, Gaillard C, Garnier C, Doublie JL (2012) Properties of cellulose/pectins composites: Implication for structural and mechanical properties of cell wall. Carbohydr Polym

90:1081–1091

4. Babbar N, Roy VS, Wijnants M, Dejonghe W, Caligiani A, Sforza S, Elst K (2016) Effect of extraction conditions on the saccharide (neutral and acidic) composition of the crude pectic extract from various agro-industrial residues. J Agric *Food Chem* 64:268–276
5. Berglund L, Breedveld L, Oksman K (2020) Toward eco-efficient production of natural nanofibers from industrial residue: Eco-design and quality assessment. J Clean Prod 255:120274
6. Browning BL (1967) Methods of wood chemistry. Volume II. Wiley, New York
7. Combo AM, Aguedo M, Quiévy N, Danthine S, Goffin D, Jacquet N, Blecker C, Devaux J, Paquot M (2013) Characterization of sugar beet pectic-derived oligosaccharides obtained by enzymatic hydrolysis. Int J Biol Macromol 52:148–156
8. Concha J, Weinstein C, Zúñiga ME (2013) Production of pectic extracts from sugar beet pulp with antiproliferative activity on a breast cancer cell line. Front Chem Sci Eng 7:482–489
9. Dinand E, Chanzy H, Vignon R (1999) Suspensions of cellulose microfibrils from sugar beet pulp. Food Hydrocoll 13:275–283
10. Fischer M, Arrigoni E, Amado R (1994) Changes in the pectic substances of apples during development and postharvest ripening. Part 2: analysis of the pectic fractions. Carbohydr Polym 25:167–175
11. Fishman ML, Chau HK, Coffin DR, Cooke PH, Qi P, Yadav MP, Hotchkiss ATJr (2011) Physico-chemical characterization of a cellulosic fraction from sugar beet pulp. Cellulose 18:787–801
12. French AD (2014) Idealized powder diffraction patterns for cellulose polymorphs. Cellulose 21:885–896
13. Fry SC (1986) Cross-linking of matrix polymers in the growing cell walls of angiosperms. Annu Rev Plant Physiol 37:165–186
14. Hassan ML, Berglund L, Hassan E, Abou-Zeid R, Oksman K (2018) Effect of xylanase pretreatment of rice straw unbleached soda and neutral sulfite pulps on isolation of nanofibers and their properties. Cellulose 25:2939–2953
15. Herrera MA, Mathew AP, Oksman K (2014) Gas permeability and selectivity of cellulose nanocrystals films (layers) deposited by spin coating. Carbohydr Polym 112:494–501
16. Hietala M, Sain S, Oksman K (2017) Highly redispersible sugar beet nanofibers as reinforcement in bionanocomposites. Cellulose 24:2177–2189
17. Holland C, Perzon A, Cassland PRC et al (2019) Nanofibers produced from agro-Industrial plant waste using entirely enzymatic pretreatments. Biomacromol 20:443–453
18. Hosseinaei O, Wang SQ, Rials TG, Xing C, Zhang Y (2011) Effect of decreasing carbohydrate content on properties of wood strands. Cellulose 18:841–850
19. Iiyama K, Lam TB-T, Stone BA (1994) Covalent cross-links in the cell wall. Plant Physiol 104:315–320
20. Fischer M, Arrigoni E, Amado R (1994) Changes in the pectic substances of apples during development and postharvest ripening. Part 2: analysis of the pectic fractions. Carbohydr Polym

25:167–175

21. Kangas H, Lahtinen P, Sneck A, Hellén E, Saariaho A-M, Laitinen O (2014) Characterization of fibrillated celluloses. A short review and evaluation of characteristics with a combination of methods. Nord Pulp Paper Res J 29:129–143
22. Kato Y, Kobayashi M (2000) Isolation and characterization of hemicelluloses from beet pulp. *J* Appl Glycosci 47:45–48
23. Leitner J, Hinterstoisser B, Wastyn M, Keckes J, Gindl W (2007) Sugar beet cellulose nanofibril-reinforced composites. Cellulose 14:419–425
24. Levigne S, Ralet MC, Thibault JF (2002) Characterisation of pectins extracted from fresh sugar beet under different conditions using an experimental design. Carbohydr Polym 49:145–153
25. Li M, Wang L-J, Li D, Cheng Y-L, Adhikari B (2014) Preparation and characterization of cellulose nanofibers from de-pectinated sugar beet pulp. Carbohydr Polym 102:136–143
26. Meseguer I, Aguilar M, González MJ, Martínez C (1998) Extraction and colorimetric quantification of uronic acids of the pectic fraction in fruit and vegetables. J Food Compos Anal 11:285–291
27. Pacheco MT, Villamiel M, Moreno R, Moreno FJ (2019) Structural and rheological properties of pectins extracted from industrial sugar beet by-products. Molecules 24:392
28. Perzon A, Jørgensen B, Ulvskov P (2020) Sustainable production of cellulose nanofiber gels and paper from sugar beet waste using enzymatic pre-treatment. Carbohydr Polym 230:115581
29. Pinkl S, Veige S, Colson J, Gindl-Altmutter W (2017) Nanopaper properties and adhesive performance of microfibrillated cellulose from different ligno-cellulosic raw materials. Polymers 9:326
30. Sàez-Plaza P, Michałowski T, Navas MJ, Asuero AG, Wybraniec S (2013) An overview of the Kjeldahl method of nitrogen determination. Part I. Early history, chemistry of the procedure, and titrimetric finish. Crit Rev Anal Chem 43:178–223
31. Schols H, Coenen G, Voragen A (2009) Revealing pectin's structure. In: Schols HA, Visser RGF, Voragen AGJ (eds) Pectins and Pectinases. Wageningen Academic Publishers, Wageningen, pp 19–34
32. Sidiras DK, Koullas DP, Vgenopoulos AG, Koukios EG (1990) Cellulose crystallinity as affected by various technical processes. Cellul Chem Technol 24:309–317
33. Siew CK, Williams PA (2008) Role of protein and ferulic acid in the emulsification properties of sugar beet pectin. J Agric Food Chem 56:4164–4171
34. Segal L, Creely JJ, Martin AE, Conrad CM (1959) An empirical method for estimating the degree of crystallinity of native cellulose using the X-ray diffractometer. Text Res J 29:786–794
35. Stevanato P, Chiodi C, Broccanello C, Concheri G, Biancardi E, Pavli O, Skaracis G (2019) Sustainability of the sugar beet crop. Sugar Tech 21:703–716
36. Thomas B, Raj M, Athira B, Rubiyah H, Joy J, Moores A, Drisko G, Sanchez C (2018) Nanocellulose, a versatile green platform: From biosources to materials and their applications. Chem Rev 118:11575–11625

37. Vartiainen J, Lahtinen P, Kaljunen T, Kunnari V, Peresin MS, Tammelin T (2015) Comparison of properties between cellulose nanofibrils made from banana, sugar Beet, hemp, softwood and hardwood pulps. O Papel 76:57–60
38. Vincken J-P, Schols HA, Oomen RJFJ, McCann MC, Ulvskov P, Voragen AGJ, Visser RGF (2003) If homogalacturonan were a side chain of rhamnogalacturonan I. Implications for cell wall architecture. Plant Physiol 132:1781–1789
39. Wathoni N, Shan CY, Shan WY, Rostinawati T, Indradi RB, Pratiwi R, Muchtaridi M (2019) Characterization and antioxidant activity of pectin from Indonesian mangosteen (Garcinia mangostana L.) rind, 5. Heliyon, p e02299
40. Wise LE, Murphy M, D'Addieco AA (1946) Chlorite holocellulose. Its fractionation and bearing on summative wood analysis and on studies on the hemicelluloses. TAPPI 29:210–218
41. Yang W, Feng Y, He H, Yang Z (2018) Environmentally-friendly extraction of cellulose nanofibers from steam-explosion pretreated sugar beet pulp. Materials 11:1160
42. Zykwinska A, Boiffard M-H, Kontkanen H, Buchert J, Thibault J-F, Bonin E (2008) Extraction of green labelled pectins and pectic oligosaccharides from plant byproducts. J Agric Food Chem 56:8926–8935
43. Zykwinska AW, Ralet MC, Garnier CD, Thibault JF (2005) Evidence for in vitro binding of pectin side chains to cellulose. Plant Physiol 139:397–407
44. Zykwinska A, Thibault J-F, Ralet M-C (2007) Organization of pectic arabinan and galactan side chains in association with cellulose microfibrils in primary cell walls and related models envisaged. J Exp Bot 58:1795–1802

Figures

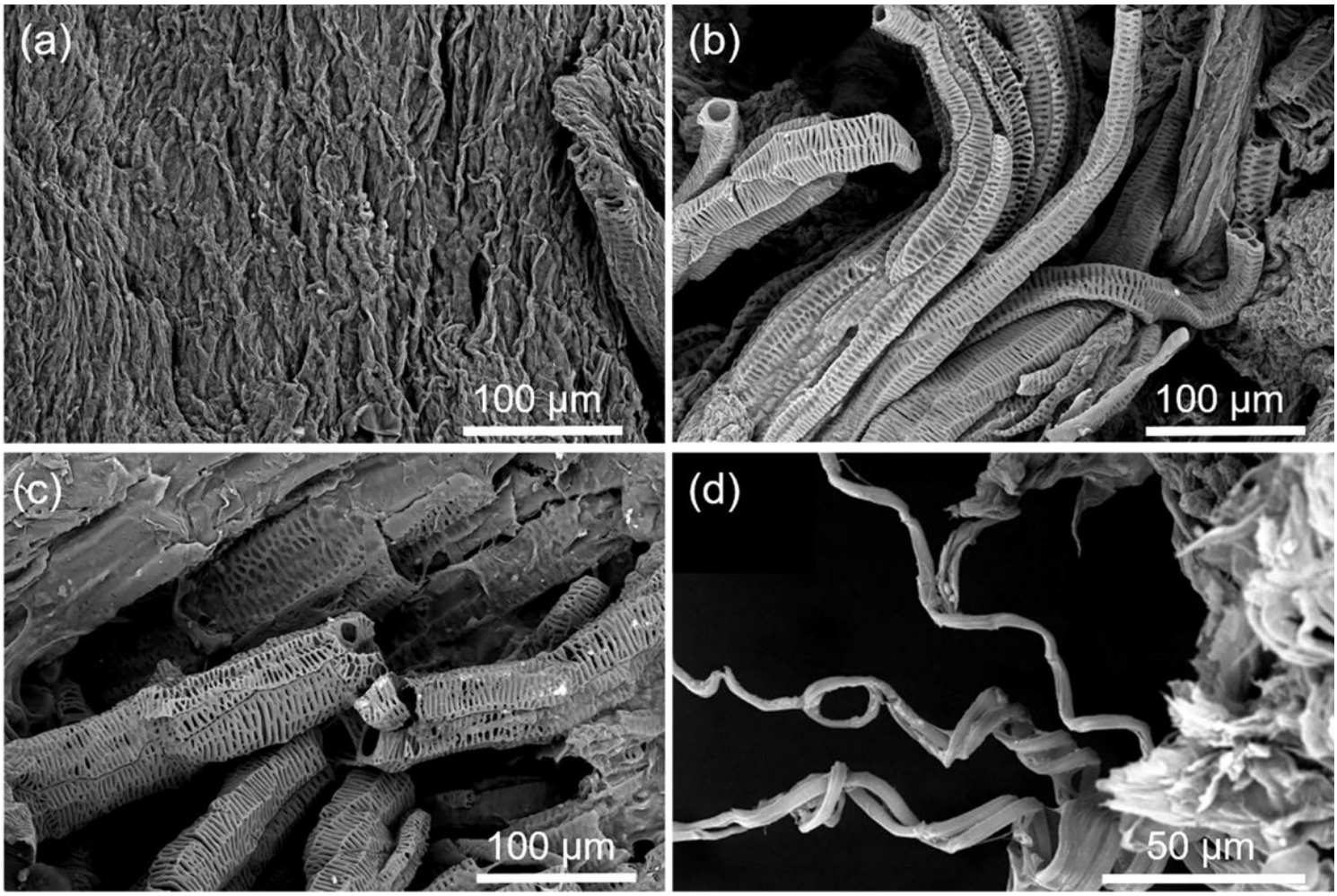

Figure 1

SEM images of SBP (a) before pectin extraction, (b) after pectin extraction with sulfuric acid at 85 °C for 2 h, (c) after pectin extraction with a 1:1.5 xylanase/cellulase enzyme mixture, and (d) after pectin extraction with sulfuric acid at 85 °C for 4 h

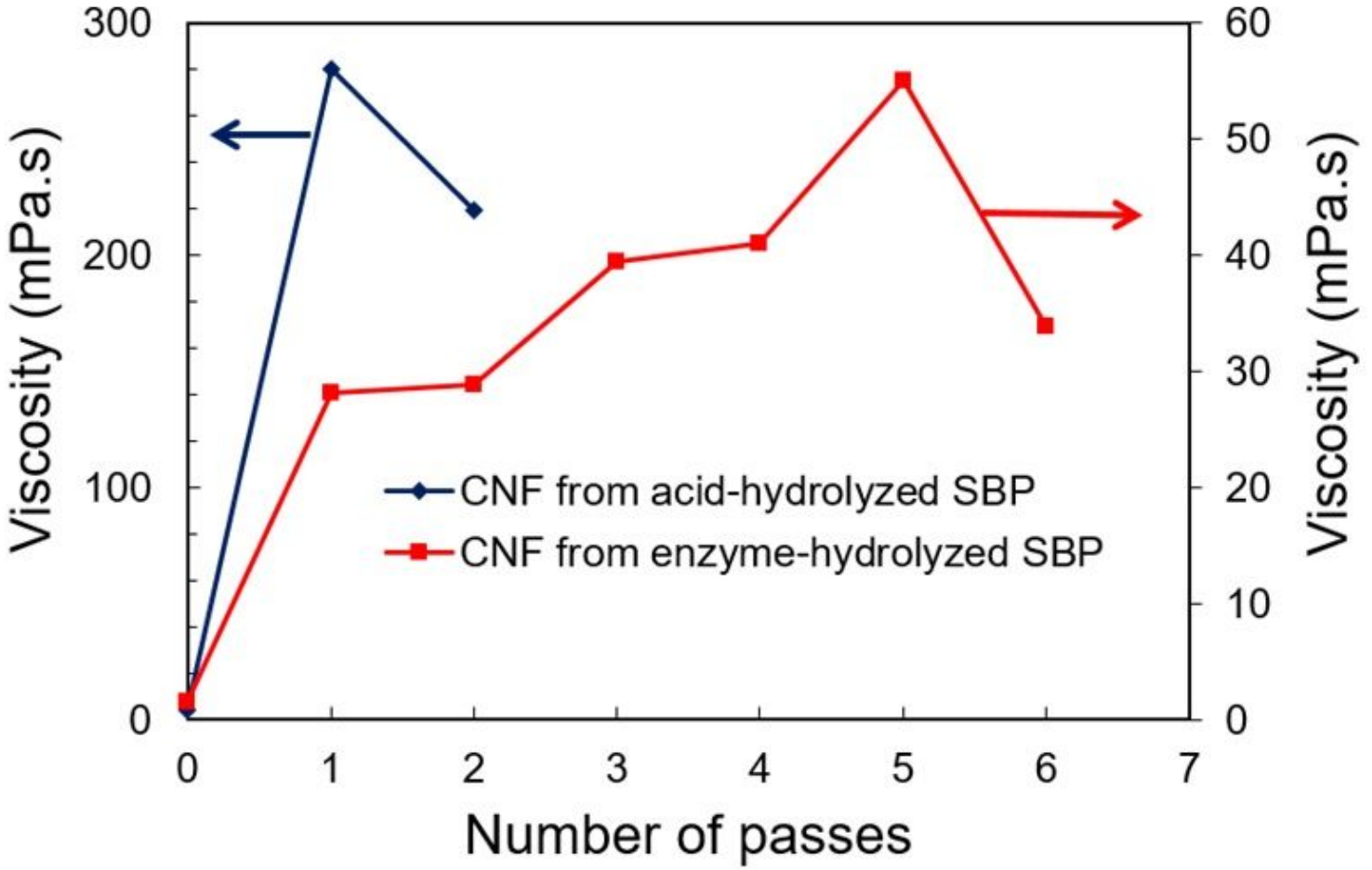

Figure 2

Effect of number of passes through the high-pressure homogenizer on viscosity of isolated nanofibers

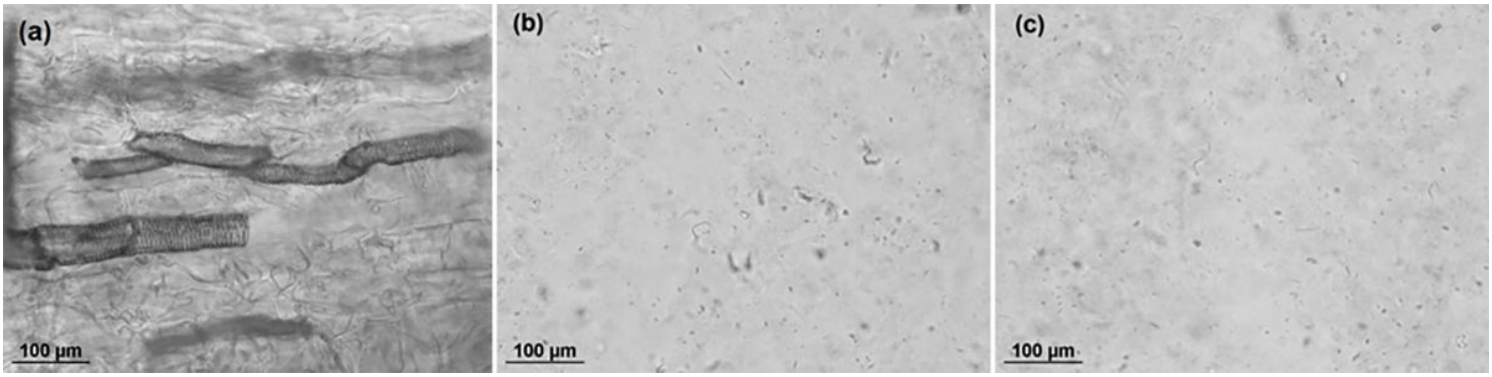

Figure 3

Optical microscopy images of acid-hydrolyzed SBP after passage through the high-pressure homogenizer (a) zero, (b) one, and (c) two times

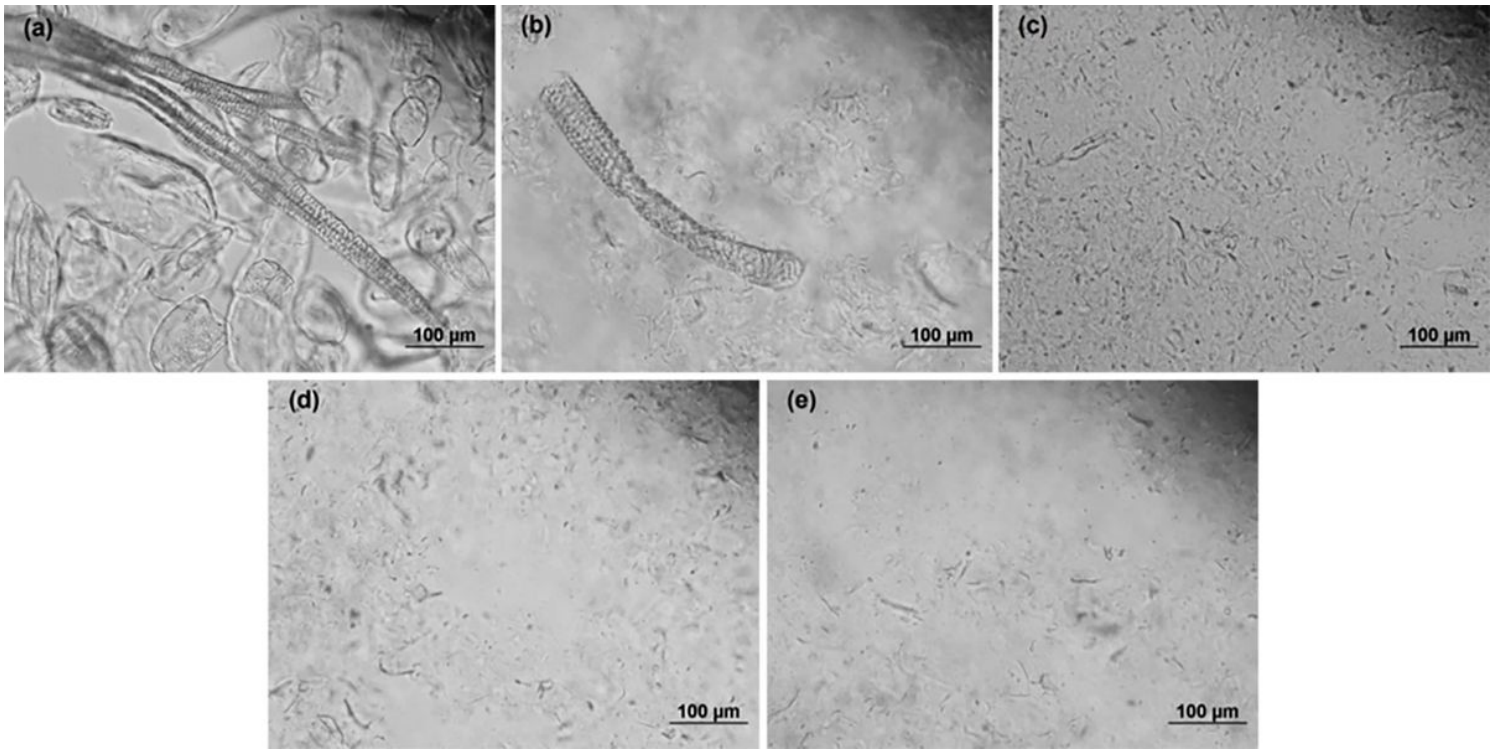

Figure 4

Optical microscopy images of enzyme-hydrolyzed SBP after passage through high-pressure homogenizer (a) zero, (b) one, (c) three, (d) five, and (e) six times

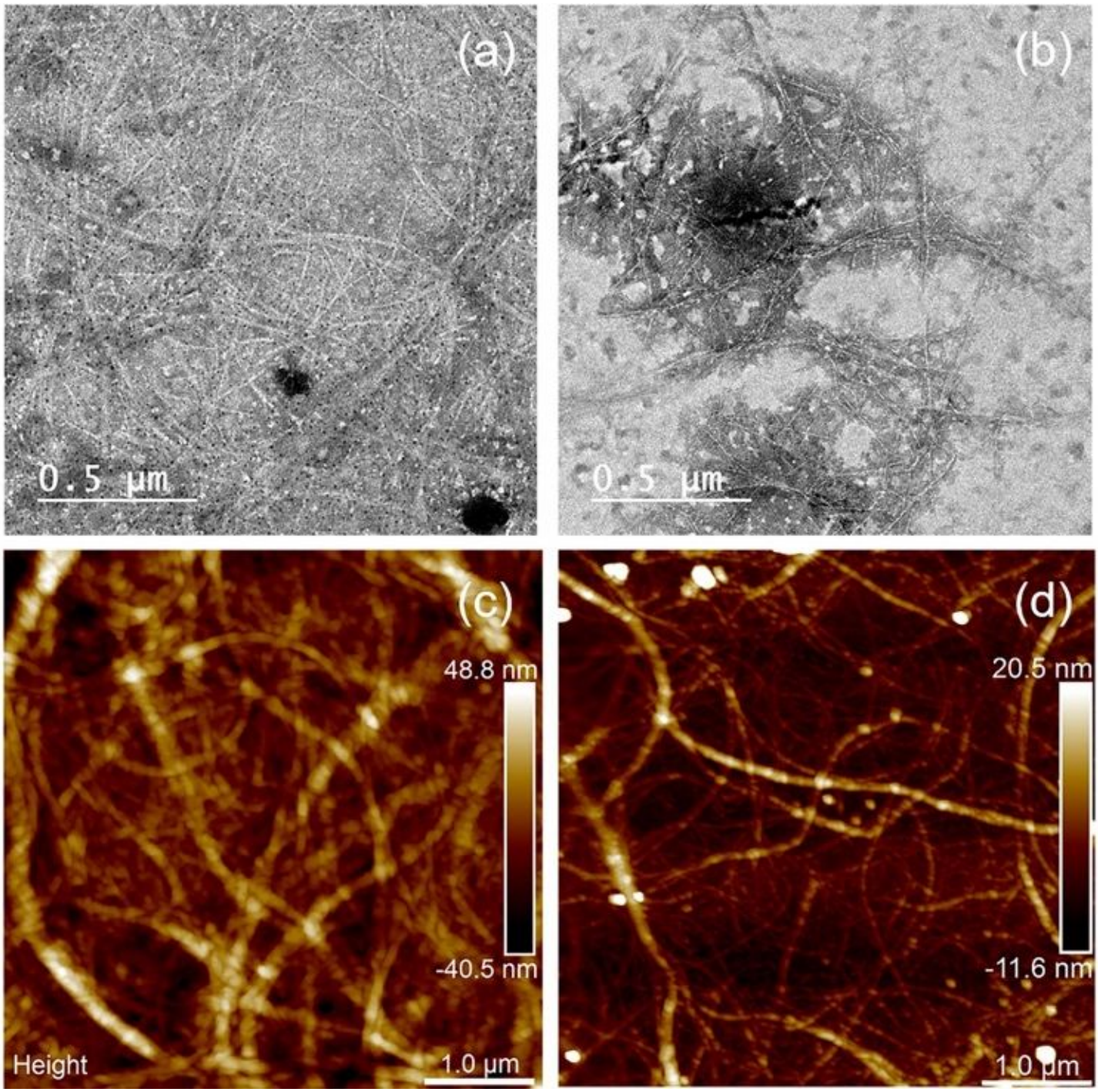

Figure 5

TEM images of CNFs isolated from (a) acid-hydrolyzed SBP and (b) enzyme-hydrolyzed SBP. AFM images in height mode of CNFs isolated from (c) acid-hydrolyzed SBP and (d) enzyme-hydrolyzed SBP

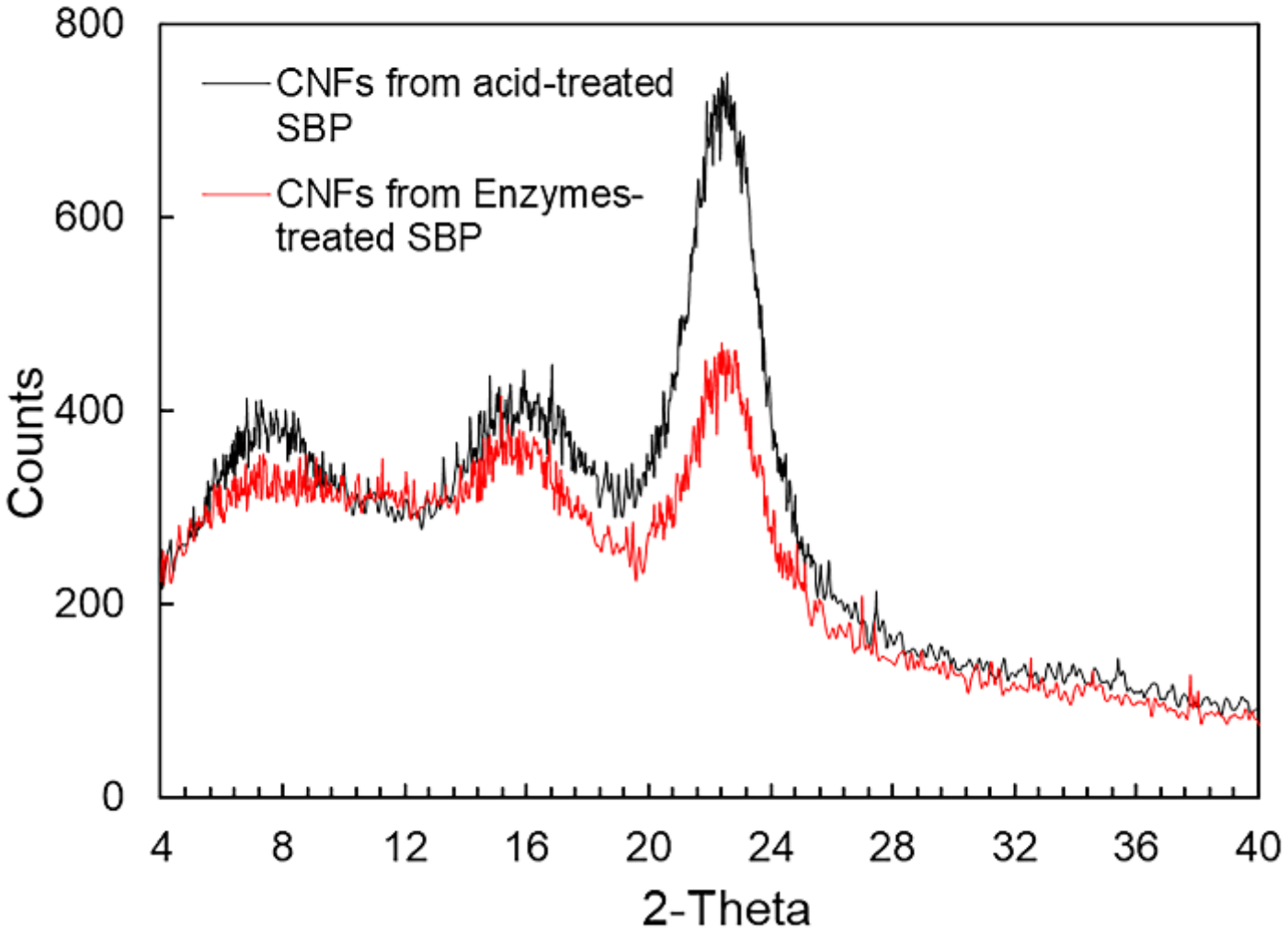

Figure 6

XRD patterns of CNFs isolated from acid- and enzyme-hydrolyzed SBP

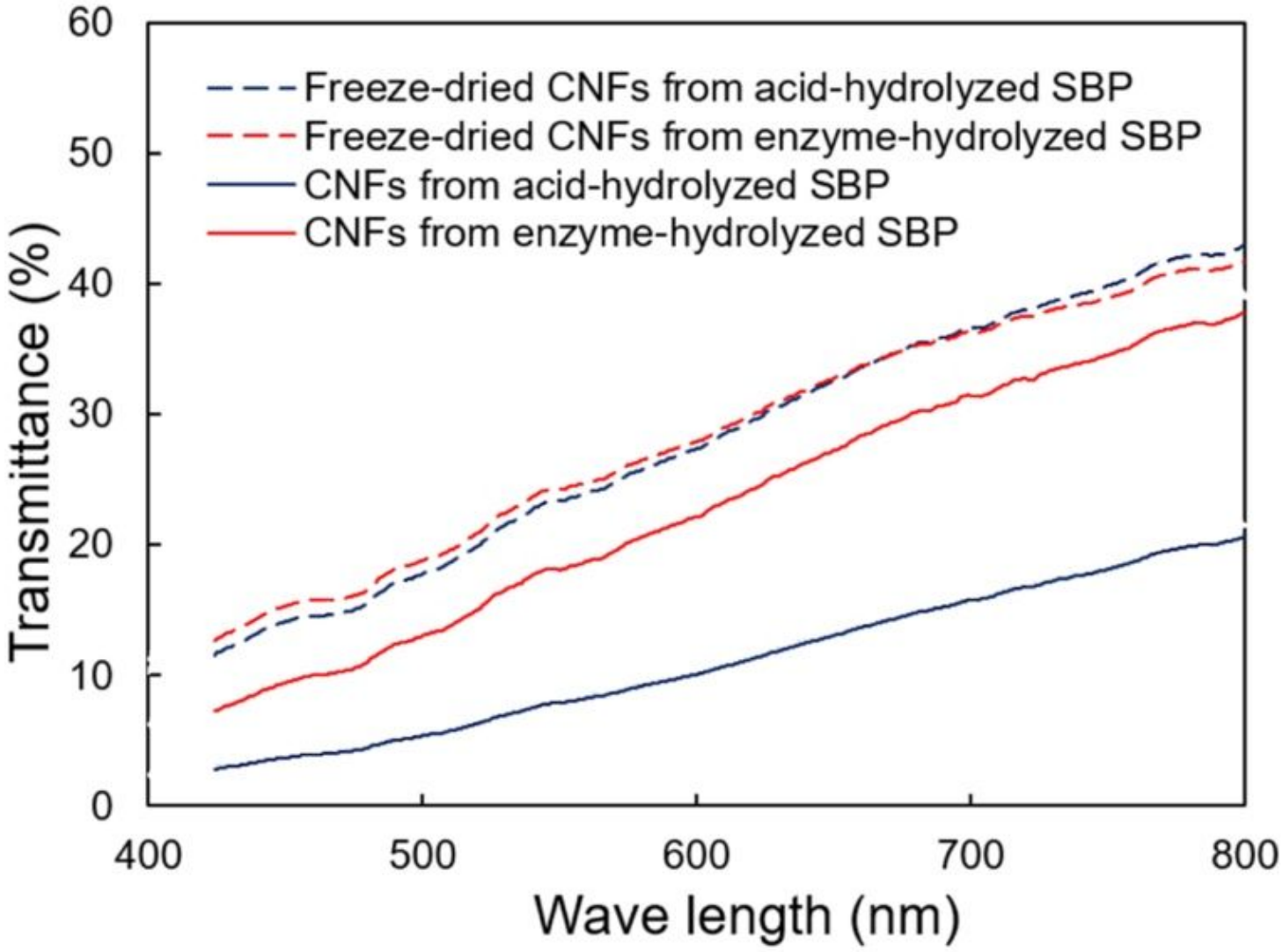

Figure 7

Light transmittance of CNFs aqueous suspensions before and after freeze-drying and redispersion in water

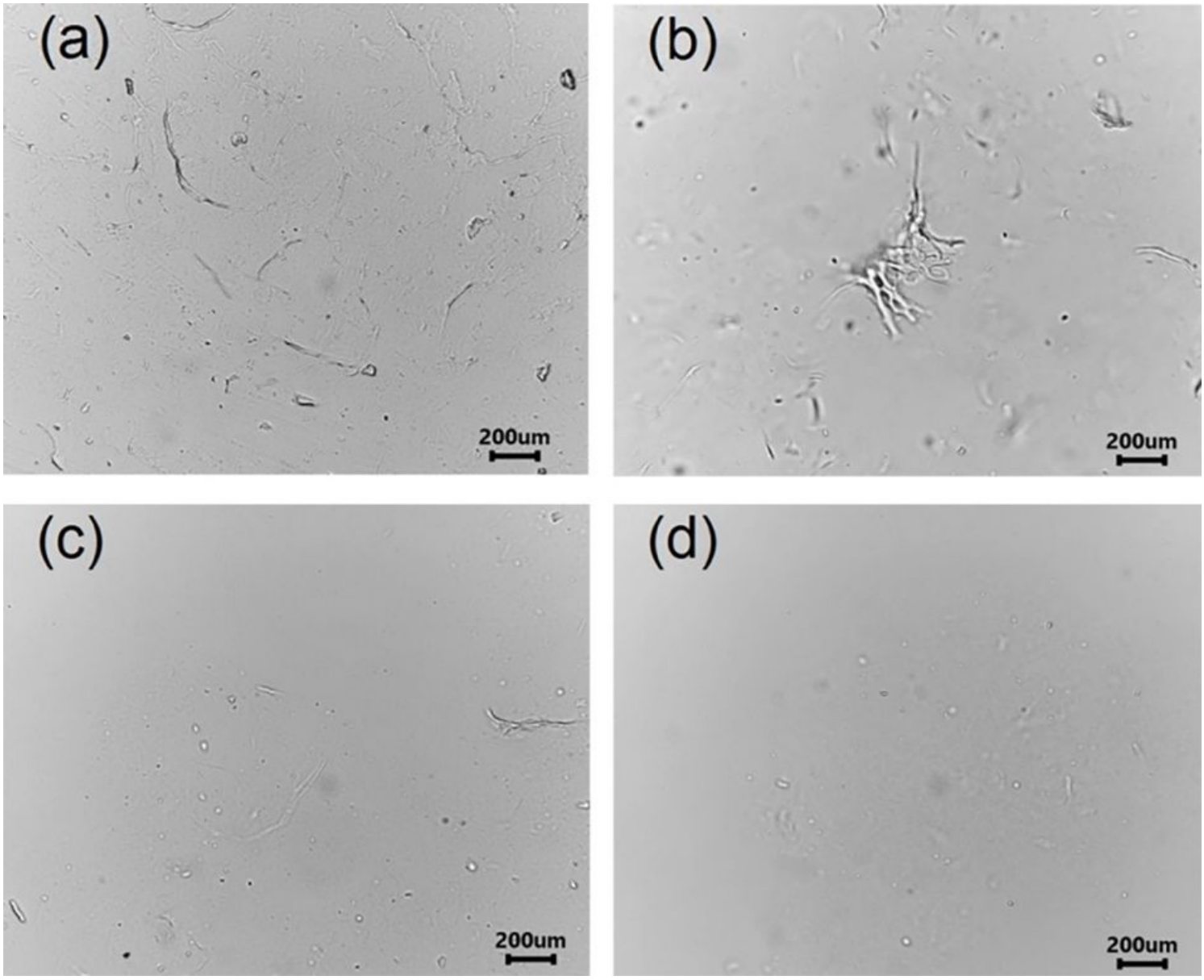

Figure 8

Optical microscopy images of redispersed CNFs isolated from (a, b) acid-hydrolyzed SBP and (c, d) enzyme-hydrolyzed SBP

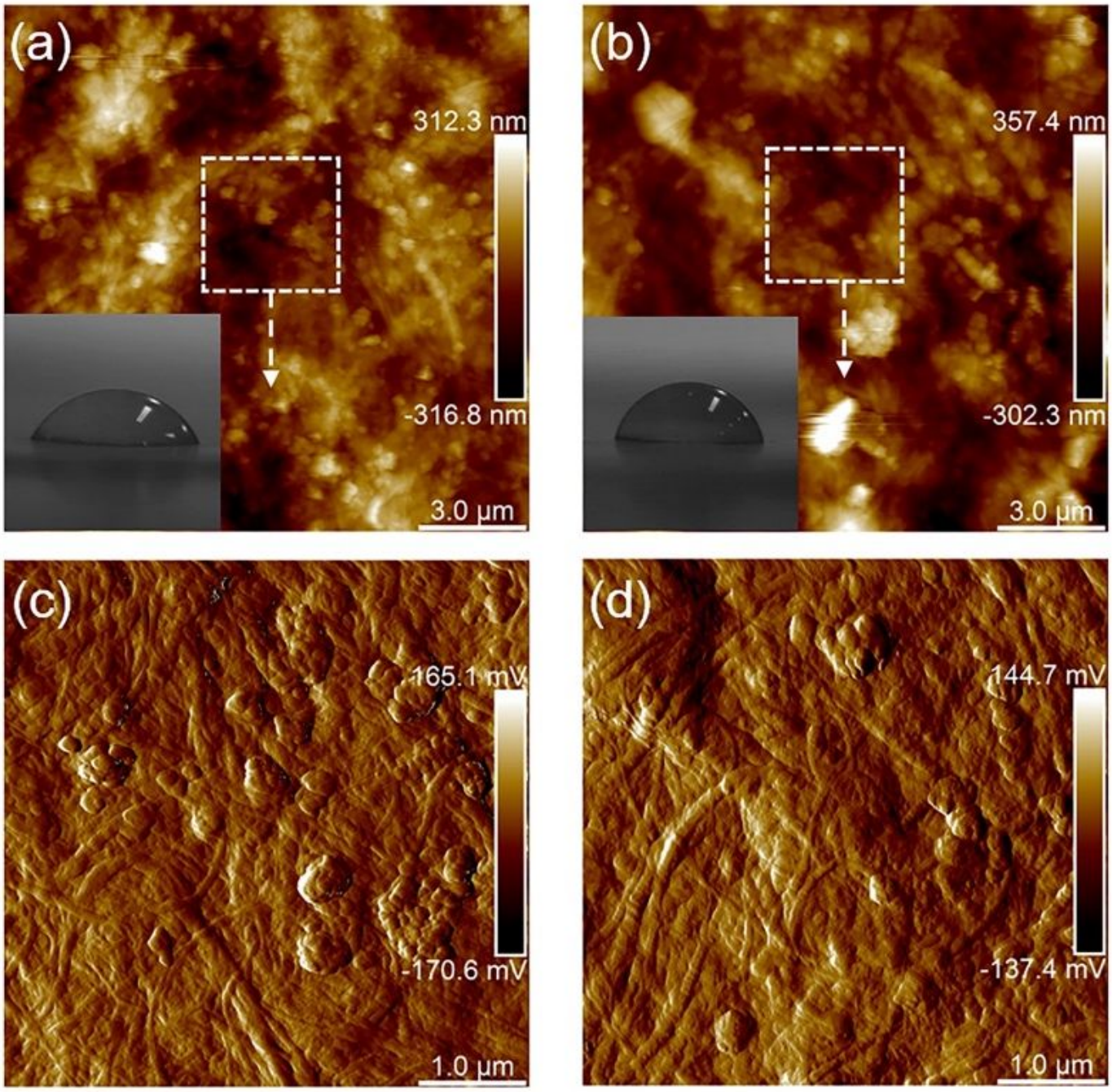

Figure 9

AFM height image images of CNFs films from (a) acid-hydrolyzed SBP and (b) enzyme-hydrolyzed SBP. Insets: Photographs of the respective water contact angles. AFM amplitude images for a smaller scan area of CNFs films from (c) acid-hydrolyzed SBP and (d) enzyme-hydrolyzed SBP

Supplementary Files

This is a list of supplementary files associated with this preprint. Click to download.

- Graphicalabstract.jpg

- SupplementaryInformationRev.docx